Analysis of Structural Factors Related to Spectroscopic Data and Redox Potentials of CuT1 Models Through DFT Tools

HUGO VÁZQUEZ-LIMA, PATRICIA GUADARRAMA

Instituto de Investigaciones en Materiales, Universidad Nacional Autónoma de México, Apartado Postal 70-360, CU, Coyoacán, México DF 04510, México

Received 6 January 2011; accepted 24 March 2011
Published online 8 May 2011 in Wiley Online Library (wileyonlinelibrary.com).
DOI 10.1002/qua.23130

ABSTRACT: Six complexes, mimics of T1 Cu active site, were studied under the density functional theory framework and their redox potentials were theoretically estimated with an average error of 0.095 V. Among different functionals, the hybrid functional PBE0 gave the best results to reproduce geometric parameters and to estimate redox potentials. The use of computational methods allowed the identification of relevant structural factors to rationalize spectroscopic and redox potential measurements. The inclusion of explicit molecules of solvent (tetrahydrofurane) showed that only those complexes with net positive charge exhibit coordination with the solvent. The consideration of such interaction permits the correct estimation of redox potentials. When the equilibrium between possible coordination isomers of T1 Cu models is taken into account, a reinterpretation of spectroscopic data (EPR and UV-vis) is possible. These equilibria are governed mainly by entropic contributions and the solvation energy. ©2011 Wiley Periodicals, Inc. Int J Quantum Chem 112: 1431–1438, 2012

Key words: DFT; redox potentials; T1 Cu site; coordination isomers; laccases

Introduction

Laccases, a family of multicopper oxidases found in bacteria, fungi, plants, and insects, have three types of copper sites, according to their spectroscopic features [1]. Particularly, the T1 Cu site, responsible for the blue color of these enzymes when oxidized, has been extensively studied, and is a recurrent motif found in proteins involved in redox processes [2]. The copper atom in this site is coordinated to two residues of histidine (His) and one of cysteine (Cys), in an unusual trigonal geometry. In some cases a fourth

Correspondence to: P. Guadarrama; e-mail: patriciagua@iim.unam.mx

Additional Supporting Information may be found in the online version of this article.

ligand (typically methionine thioether) is present at long distances (2.6–2.9 Å).

Many efforts have been made, from different angles, to try to understand the action mechanisms of active sites of copper. A strategy has been the inclusion of those main features of active sites in synthetic models to achieve a deeper understanding from the structural and electronic standpoint.

In this regard, Holland and Tolman have made significant contributions with the synthesis of the first Cu^{2+}-complex with trigonal-planar structure, including a thiolate moiety that mimics the trigonal T1 Cu site present in laccases of high redox potential [3, 4]. After spectroscopic characterization, the trigonal planar geometry, similar to that observed for the proteinic three-coordinate T1 Cu site, was confirmed.

Despite the structural similarity, the redox potential of the synthetic models measured in tetrahydrofurane (THF) is much lower ($E_{1/2} = -0.18$ V vs. NHE), when compared with the tricoordinated fungal laccase ($> +0.7$ V), presumably due to the charge donation by the anionic ligands. Later on, another tricoordinated copper model, including a histidine-cysteine bridged dicopper array, was prepared, characterized, and its redox potential was measured by cyclic voltammetry [5]. Low values are reported: -0.986 and -0.108 V (vs. Fc/Fc^{+}). One of the most important contributions of the synthetic models described so far is the generation of experimental electrochemical data, directly related with the most important application of this kind of systems: the catalytic oxidation of several harmful substrates [6] with the concomitant reduction of O_2 to H_2O. Cyclic voltammetry provides an experimental means for the measurement of redox potentials when the electron-transfer process is reversible. In this sense, additional data were obtained from voltammetry experiments on novel three-coordinated Cu^{2+}-phenolates, isolated and characterized [7]. The observed negative potentials are consistent with the expected electron donating effect of the ligands, stabilizing preferably the oxidized state of the metal.

From the theoretical point of view, the experimental information is a valuable source of feedback to validate methods. Using quantum chemistry tools is possible to reproduce redox potentials and get further information regarding structural characteristics that can be missed by spectroscopic common tests. Ultimately, the theoretical calculations can acquire a predictive character on other new active molecular systems.

Different theoretical approximations based on LUMO energies, electron affinities in gas phase or free energies in solution have been employed to estimate redox potentials. Also the inclusion of available experimental data (solvation energies or ionization potentials in gas phase) to the calculations has been used [8]. Whatever the approximation chosen, the values obtained are generally validated by plotting the experimental data versus the calculations. An acceptable methodology will generate a slope close to 1; the closest to 1 is this value, the higher the quality of the methodology to estimate redox potentials.

If a good quality of the methodology to calculate redox potentials is assured, other issues like the role played by the surroundings of T1 Cu site on the redox potential of the protein can be addressed with greater certainty to ultimately try to answer intriguing questions [9] like: Why several proteins containing active sites like T1 Cu, having the same spectroscopic patterns, have different redox potentials?

In this study, based on the DFT level of theory, the experimental redox potentials of six complexes mimics of the T1 Cu active site were reproduced in solution, following a methodology that allows an average error of 0.095 V. Taking advantage of quantum chemistry tools, a deeper insight into some structural characteristics was also addressed, underlining some peculiarities not explained spectroscopically, that might have impact on the experimental interpretation as well as on the redox potentials measurements.

Methods

Six copper models previously synthesized (**A**-**F**, Fig. 1) were taken into account in the present study [3–5, 7].

Among the DFT functionals M05, B3LYP, BP86, and PBE0 [10], it was previously determined that PBE0 reproduces quite well the most important crystallographic distances in copper complexes, in combination with LACVP** basis set [11, 12]; thus all the copper models (**A** to **F**) in both copper oxidation states, Cu^{+} and Cu^{2+}, were fully optimized at PBE0/LACVP** level included in Jaguar program version 7.0 [13]. As the experimental determinations of redox potentials were made in THF as solvent, the optimizations were also carried out in the presence of explicit molecules of THF to

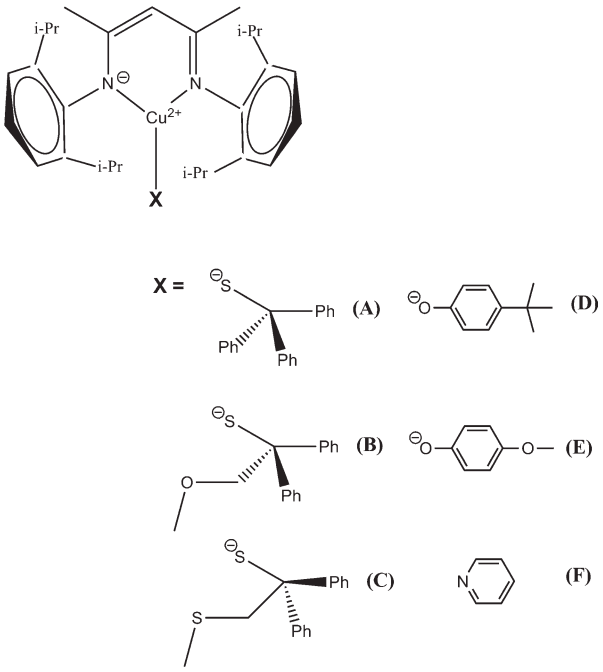

FIGURE 1. Synthetic models reported by Tolman.

discard or confirm a possible complexation of solvent molecules to copper. The redox potential calculations were carried out according to the thermodynamic cycle shown later [14], where the ferrocene/ferrocenium (Fc/Fc^+) redox pair was taken as reference system.

The solvation energies were calculated with the Poisson-Boltzmann model [15, 16] to obtain the free energies in solution as:

$$\Delta G^o_{Sol} = \Delta G^o_g + \Delta G^o_{Solv(Cu+)} + \Delta G^o_{Solv(Ferrocenium)} - \Delta G^o_{Solv(Cu2+)} - \Delta G^o_{Solv(Ferrocene)} \quad (1)$$

To eventually calculate the redox potentials as:

$$E^o = \Delta G^o_{Sol}/nF \quad (2)$$

where n is the number of transferred electron and F is the Faraday constant. As the reference value of Fc/Fc^+ is included in Eq. (1), there is no need to add any other reference in Eq. (2).

Results and Discussion

Table I shows the geometric deviations between fully optimized structures and the crystallographic ones.

From Table I, DFT gives a rather good description, within the acceptable error for metallic complexes [17]. In general, Cu—N distances from the ligand are better reproduce than Cu—X distances from the substituents. In case of complex **B**, after full optimization are observed two minima energetically separated by 2 kcal/mol [(a) and (b) in Fig. 2], whose main difference is the distance between the copper and the oxygen of the pendant substituent.

Even though the structure of minor energy corresponds to the complex where the pendant ether is coordinated to the Cu^{2+} ion [structure (b) in the figure], the structure (a) and the crystallographic structure coincide better. Thus, the geometric validation in this case was made taking into account not the global minimum structure but the other minimum [structure (a)] most related with the crystallographic structure.

The optimization of the complexes in the presence of explicit molecules of solvent (THF)

TABLE I

Deviation of distances (in Å) of fully optimized structures of complexes A-F at PBE0/LACVP level versus crystallographic data.**

	Cu-N (1)			Cu-N (2)			Cu-X ; X = S, O or N			Cu—S from tioether		
X	Crystal	PBE0	Difference	Crystal	PBE0	Difference	Crystal	PBE0	Difference	Crystal	PBE0	Difference
(A) $S(CPh_3)$	1.921	1.950	−0.029	1.923	1.964	−0.041	2.124	2.190	−0.066			
(B) $S(CPh_2CH_2OCH_3)$	1.900	1.950	−0.050	1.908	1.962	−0.054	2.119	2.190	−0.071			
(C) $S(CPh_2CH_2SCH_3)$	1.952	1.992	−0.040	1.987	2.024	−0.037	2.242	2.295	−0.053	2.403	2.554	−0.151
(D) OPh-*t*-Butyl	1.869	1.906	−0.037	1.896	1.950	−0.054	1.817	1.835	−0.018			
(E) OPh-OMethyl	1.864	1.911	−0.047	1.888	1.957	−0.069	1.806	1.838	−0.032			
(F) Pyridine[a]	1.947	1.970	−0.023	1.947	1.993	−0.046	1.947	1.993	−0.046			

[a] Complex **F** is the only one whose crystallographic structure corresponds to Cu^+.

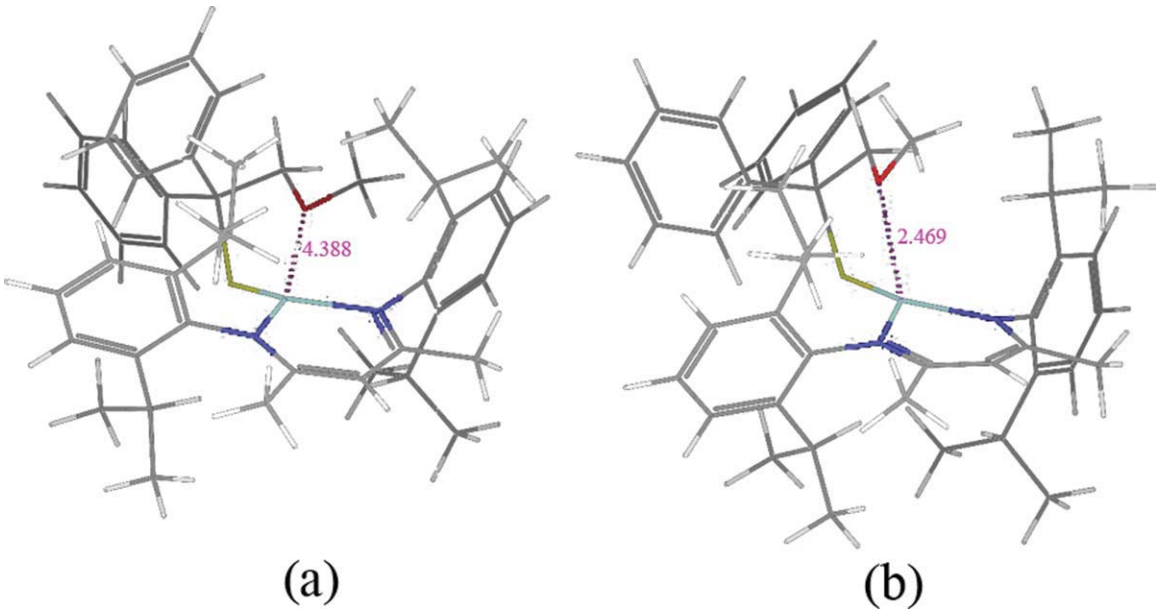

FIGURE 2. Two minima obtained for complex **B**. (a) tricoordinated complex, (b) tetracoordinated complex. Cu—O_{ether} distances (Å) are shown in pink. [Color figure can be viewed in the online issue, which is available at wileyonlinelibrary.com.]

suggests that the coordination between the oxygen of the THF and the copper turns out to be poorly favored, except for oxidized complex **F** with X = pyridine, where the Cu—O_{THF} distance is 2.21 Å, which could affect the redox potential. Figure 3 shows the Cu^{2+} coordination with one molecule of THF on complex **F**, in contrast with that observed for other complexes (for example complex **D**) where the molecules of THF interact in a very weak way, only at dipole–dipole level, similar to what might happen between molecules of THF themselves.

To quantify the interaction Cu—O_{THF}, the interaction energies for all complexes were calculated and corrected due to the basis set superposition error (BSSE) by the Counterpoise protocol [18] (see Supporting Information).

For complexes **A**-**E**, the corrected interaction energies are equivalent to dipole–dipole and ion-dipole interactions (around 1–3 kcal) but in case of complex **F**, a sum of coordination and ion-dipole interactions for Cu^{2+} is observed ($E_{interaction}$ = −7.29 kcal/mol), where ~6 kcal/mol can be attributed to a coordination interaction (only with one molecule of THF) and the rest to ion-dipole and dipole–dipole interactions.

Therefore, the solvation energies and the subsequent calculation of redox potentials were done in absence of explicit molecules of solvent, except for complex **F**.

Redox Potential Calculations

Following the thermodynamic cycle from Scheme 1, and starting with the optimized geometries, single point frequency calculations at PBE0/LACVP**++ level were carried out to obtain ΔG_g^o values. Optimization calculations in solution (Poisson-Boltzmann model) were carried out to obtain ΔG_{Sol}^o values. It should be mentioned that in these calculations are included diffuse basis (++) for better energy estimation. According to the equations 1 and 2 mentioned before, the redox potentials (E^o) were calculated (see Table II).

The followed methodology allows obtaining a maximum deviation of 0.149 V from experimental data. The reproduction of redox potentials versus ferrocene in different nonaqueous solvents can have errors as high as 0.16 V [8]; the highest error from Table II is below this value. Other parameters such as average error and the slope of the curve obtained by plotting calculated versus experimental data indicate a good correlation between experiment and calculations (see later).

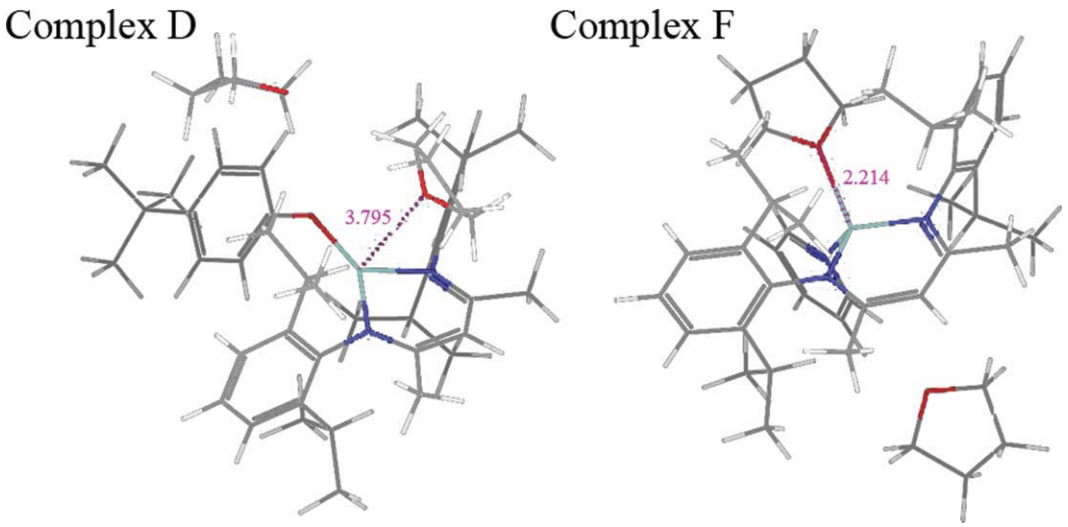

FIGURE 3. Two forms of THF interaction with the studied complexes. Left: no coordination interaction between complex **D** and THF. Right: coordination interaction between complex **F** and THF. Cu—OTHF distances (Å) are shown in pink. [Color figure can be viewed in the online issue, which is available at wileyonlinelibrary.com.]

To explore a possible improvement of the calculated redox potential, besides PBE0, other functionals like BP86, M05, B3LYP and a hybrid functional proposed by Szilagyi et al. [19] were tested with the basis set LACVP**++ to carry out single point calculations to obtain the electronic energies in gas phase. The solvation energies were also calculated with several functionals but practically the same results are obtained.

Thus, taking into account the zero point energies previously calculated with PBE0 (according to the procedure followed by Cramer-Truhlar [20]) to obtain ΔG°_{g}, and the solvation energies also calculated with PBE0, the redox potentials were estimated with different functionals and the values were graphed against experimental data to use the slopes as criterion of good correlation [8] (see Fig. 4).

The calculated slop on each case, as well as the average error (obtained as the average of the difference between experimental and calculated redox potential of each complex) are shown in Table III.

According to Table III, the best correlation is obtained by the functional proposed by Szilagy. M05 and PBE0 provide a slight deviation from the ideal behavior (slope = 1); B3LYP and BP86 have the largest deviation among the functionals tested but still provide a good reproduction. Regarding the average error, PBE0 offers the minimum value. Taking into account both parameters, PBE0 was selected as the more suitable functional for redox potentials estimation for the series of complexes under study.

Taking advantage of the simulations, different coordination isomers can be recognized for the same complex, as will be shown later, varying

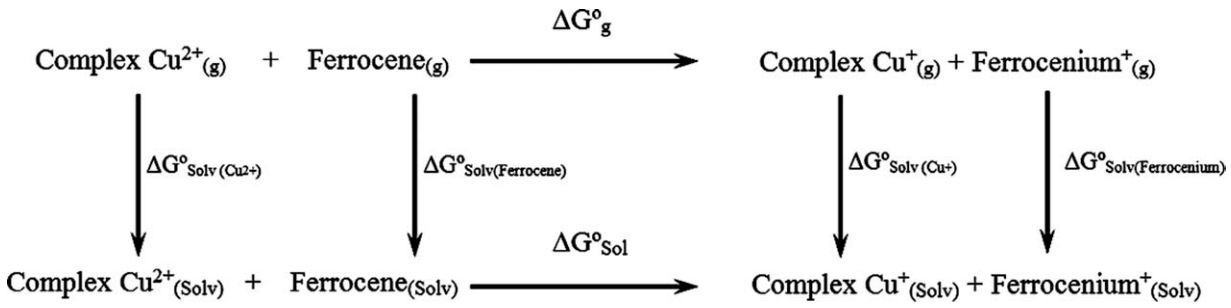

SCHEME 1. Thermodynamic cycle; ΔG°_{g} = free energy variation in gas phase; ΔG°_{Solv} = Solvation energy of gas phase species; ΔG°_{Sol} = free energy variation in solution.

TABLE II

Redox potential calculations at PBE0/LACVP++ level.**

Complex	A	B	C	D	E	F
ΔG^{o}_{g} (kcal/mol)	85.0	82.9	83.4	87.4	89.5	13.7
$\Delta G^{o}_{Solv(CuI)} + \Delta G^{o}_{Solv(Ferrocenium)}$ (kcal/mol)	−74.4	−76.5	−77.2	−76.5	−79.5	−50.6
$\Delta G^{o}_{Solv(CuII)} + \Delta G^{o}_{Solv(Ferrocene)}$ (kcal/mol)	−12.2	−13.1	−13.4	−11.2	−12.2	−36.2
ΔG^{o}_{Sol} (kcal/mol)	22.9	19.4	19.6	22.1	22.3	−0.6
E° calculated (Volts)	−0.991	−0.843	−0.851	−0.958	−0.966	0.028
E° experimental (Volts)	−0.986	−0.920	−1.000	−1.080	−1.060	−0.108
Difference (Volts)	0.005	−0.077	−0.149	−0.122	−0.094	−0.136

only by a few kcal/mol in energy, and interestingly, these coordination isomers can be correlated with experimental observations.

From Figure 1, complexes **B** and **C** exhibit two possible coordination isomers in both copper oxidation states, I and II (see Supporting Information), corresponding to the occurrence or not of a complexation between copper and the flexible moieties of methylether (complex **B**) or methyltioether (complex **C**) to achieve either a tricoordinated or a tetracoordinated arrangement. The predominance of one of the arrangements can be related with spectroscopic properties and redox potentials. The energy of each coordination isomer may be influenced by several factors including: (i) steric hindrance (the voluminous main ligand was intended to favor the tricoordination, thus the tetracoordination should be marginal); (ii) number of ligands (in case of Cu^{2+}, the tetracoordination increases the cation stability; (iii) entropic contribution (the tetracoordination diminishes the degrees of freedom of the complex and therefore the entropic contribution to the free energy; and (iv) solvent polarization (the complex that achieves a better polarization of the medium will turn out to be benefited by the solvation energy).

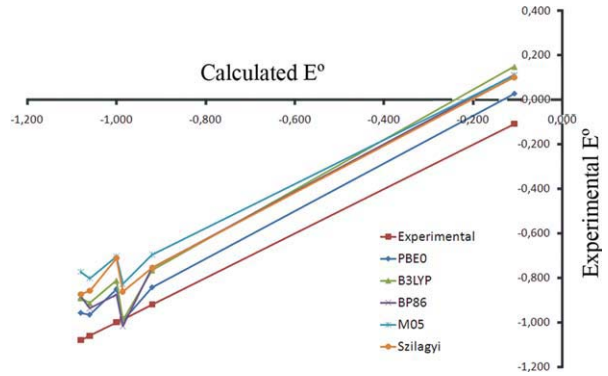

FIGURE 4. Redox potentials reproduction by different DFT functionals. [Color figure can be viewed in the online issue, which is available at wileyonlinelibrary.com.]

The coexistence of the tri and tetracoordination was evaluated by Boltzmann distributions in three different scenarios: (1) at low temperature (20 K) since experiments like EPR takes place at these temperatures; (2) at room temperatures to correlate with UV-vis experiments; and (3) at room temperature in solution (THF) to correlate with redox potential measurements. The calculated distributions are shown in Table IV.

As expected for complexes **B** and **C** with Cu^{+} (net charge of −1), additional electron pairs from extra ligands are naturally repelled, thus the tetracoordination is not favored; nevertheless, in the presence of a polarizable medium like the continuum solvent, a small percentage of tetracoordination appears since the charges repulsion can, in some way, be assimilated by the distortion of such medium.

In case of Cu^{2+} complexes, when the solvation is involved, the tricoordination is favored presumably because the tetracoordination reduces the cation exposition to the solvent, decreasing its polarization, in contrast to what happen in the tricoordinated complexes.

When the Boltzmann distributions are estimated at different temperatures, the populations

TABLE III

Slops and average error (V) for each functional in the calculation of redox potentials.

Funcional	Slop	Average error
PBE0	1.05	−0.10
B3LYP	1.12	−0.16
BP86	1.11	−0.13
M05	0.95	−0.24
Szilagyi	1.01	−0.20

TABLE IV

Boltzmann distributions[a] for complexes B and C in vacuum at 20 K, 298 K and in solution (THF) at 298 K.

	Oxidation state	Coordination number	% in vacuum at 20 K	% in vacuum at 298 K	% in THF at 298 K
Complex B	Cu I	4	0.000	0.002	12.060
		3	100.000	99.998	87.940
	Cu II	4	0.000	7.718	1.991
		3	100.000	92.282	98.009
Complex C	Cu I	4	0.000	0.010	0.001
		3	100.000	99.990	99.999
	Cu II	4	100.000	48.807	27.067
		3	0.000	51.193	72.933

[a] Boltzmann distribution were calculated with the formula: $\frac{N_i}{N} = \frac{g_i \exp(-E_i/kT)}{\sum_j g_j \exp(-E_j/kT)}$

g_i: degeneration state of the ith state; $g = 1$ in the studied cases.
E_i : Energy of the ith state; substituted by G_{THF} (298°K), G_{Vacuum} (298°K) or G_{Vacuum} (20°K) in each case.
k: Boltzmann constant.
T: Temperature.

depend on the variation of the entropic term –TS of the Gibbs free energy. In case of complex **C** with Cu^{2+}, a decrement in temperature favors the tetracoordination. In terms of energy, the free energy difference between tetra and tricoordinated complex ($\Delta G_{\text{tetracoordination-tricoordination}}$) is 0.3 kcal/mol at 298 K and −1.5 kcal/mol at 20 K, denoting a major stabilization of tetracoordinated complex at lower temperatures. Thus, even though the tetracoordination stabilizes the Cu^{2+} cation, the entropic contribution at 298 K of the tricoordinated complex is enough to equal the populations in vacuum.

For complex **B** Cu^{2+}, although the $\Delta G_{\text{tetracoordination-tricoordination}}$ difference decreases at lower temperatures (from 1.5 kcal/mol at 298 K to 0.8 kcal/mol at 20 K), the population of tetracoordination goes down and the tricoordination prevails. When two states with different energy are present, the probability that the most destabilized state contributes to the total Boltzmann population decreases as the temperature descends; thus, in this case the probability to find the complex in a local minimum with energy higher than a global minimum decreases as the temperature falls down.

It is important to underline that the tricoordinated species are always the predominant ones in solution (THF), thus the possible equilibrium with the tetracoordinated complexes might not be relevant for redox potential calculations; however, is of interest to explain some spectroscopic aspects of complexes **B** and **C** [4]. The UV-vis absorption spectra for the complexes **A**, **B**, and **C** show maxima in $\lambda_{max} = 749$ nm ($\varepsilon = 5{,}800$), $\lambda_{max} = 738$ nm ($\varepsilon = 5{,}600$), and $\lambda_{max} = 538$ nm ($\varepsilon = 2{,}100$) and $\lambda_{max} = 691$ nm ($\varepsilon = 2{,}300$), respectively. The experiments were carried out at room temperature in nonpolar solvents (heptanes, pentane and toluene), which might be related with the Boltzmann distributions in vacuum at 298 K from Table IV. From the experiment is discussed that the maxima for complexes **A** and **B** are very similar as the tricoordinated structure of both complexes is comparable. In the estimated Boltzmann distribution for complex **B**, there is a patent dominance of the tricoordinated specie (more than 90%) which agrees quite well with the experimental observation. On the other hand, in case of complex **C** two absorption maxima of similar intensity in the UV-vis spectrum were observed. In general this kind of absorptions is attributed to the ligand-metal charge transfer ($S \rightarrow Cu^{2+}$). Experimentally these absorption bands were explained as the Cu-S distance elongation, with the concomitant decrement of charge transfer, due to the tetracoordination. From the calculations, this complex exhibited equivalent Boltzmann weighting for tri and tetracoordination at room temperature (see Table IV). Since the surroundings of the sulfur atom from thiolate groups are different in each case, the two maxima experimentally observed might be explained by the occurrence of both coordination isomers.

Regarding the EPR experiments carried out at low temperatures, as was mentioned before, they can be related with calculations at 20 K showed in Table IV. In these conditions, complex **B** is found exclusively as tricoordinated while complex **C** as tetracoordinated, which is in excellent agreement with that observed experimentally [4] where only appear signals for one specie: the tricoordinated for complex **B** and tetracoordinated for complex **C**.

These theoretical precisions about the predominant coordination number allow us to state that even though the spectroscopies assign the tetracoordination for complex **C**, the redox potential in THF actually was determined for the tricoordinated specie.

Conclusions

Redox potentials of synthetic mimics of T1 Cu site were theoretically reproduced with an average error of 0.095V. Within DFT framework, different functionals were tested and the best results in both, geometric description and redox potentials estimation was the hybrid functional PBE0.

The use of computational methods allows the incorporation of solvent explicit molecules (THF) and, as a result, it was possible to identify that only those complexes with net positive charge exhibit coordination with the solvent. This is the case of oxidized complex **F**.

The interpretation of spectroscopic data must be complemented with the analysis of possible coordination isomers, as was corroborated for complexes **B** and **C**. In these two cases, the entropic contributions and the solvation energy modify the equilibrium of the coordination isomers when different conditions are used as occur in different spectroscopies (EPR and UV-vis) or redox potentials determinations. Thus, the coexistence of coordination isomers seems to be responsible of the appearance of UV-vis spectra, and not the Cu-S distance elongation, as was established before.

ACKNOWLEDGMENTS

The authors acknowledge the support of DGSCA, UNAM, for the use of the supercomputer KanBalam and CONACYT for doctoral scholarship.

References

1. Palmer, A. E.; Randall, D. W.; Xu, F.; Solomon E. I. J Am Chem Soc 1999, 121, 7138.
2. Solomon, E. I.; Szilagyi, R. K.; George, S. D.; Basumallick, L. Chem Rev 2004, 104, 419.
3. Holland, P. L.; Tolman, W. B. J Am Chem Soc 1999, 121, 7270.
4. Holland, P. L.; Tolman, W. B. J Am Chem Soc 2000, 122, 6331.
5. Lee, W.-Z; Tolman, W. B. Inorg Chem 2002, 41, 5656.
6. Shleev, S. V.; Morozova, O. V.; Nikitina, O. V.; Gorshina, E. S.; Rusinova, T. V.; Serezhenkov, V. A.; Burbaev, D. S.; Gazaryan, I. G.; Yaropolov, A. I. Biochimie 2004, 86, 693.
7. Jazdzewski, B. A.; Holland, P. L.; Pink, M.; Young, V. G.; Spencer, D. J.; Tolman, W. B. Inorg Chem 2001, 40, 6097.
8. Evans, D. H. Chem Rev 2008, 108, 2113.
9. Quintanar, L.; Stoj, C.; Taylor, A. B.; Hart, P. J.; Kosman, D. J.; Solomon, E. I. Acc Chem Res 2007, 40, 445.
10. Adamo, C.; Barone, V. J Chem Phy 1999, 110, 6158.
11. Hay, P. J.; Wadt, W. R. J Chem Phys 1985, 82, 270.
12. Vázquez-Lima, H.; Guadarrama, P.; Martínez-Anaya, C. J Mol Model (in press).
13. Jaguar, version 7.0, Schrödinger, LLC, New York, NY, 2007.
14. Felton, G. A.; Vannucci, A. K.; Chen, J.; Lockett, L. T.; Okumura, N.; Petro, B. J.; Zakai, U. I.; Evans, D. H.; Glass, R. S.; Lichtenberger, D. L. J Am Chem Soc 2007, 129, 12521.
15. Marten, B.; Kim, K.; Cortis, C.; Friesner, R. A.; Murphy, R. B.; Ringnalda, M. N.; Sitkoff, D.; Honig, B. J Phys Chem 1996, 100, 11775.
16. Tannor, D. J.; Marten, B.; Murphy, R.; Friesner, R. A.; Sitkoff, D.; Nicholls, A.; Ringnalda, M.; Goddard, W. A., III; Honig, B. J Am Chem Soc 1994, 116, 11875.
17. Solomon, E. I; Gorelsky, S. I.; Dey A. J Comput Chem 2006, 27, 1415.
18. Boys, S. F.; Bernardi, F. Mol Phys 1970, 19, 553.
19. Szilagyi, R. K.; Metz, M.; Solomon, E. I. J Phys Chem A 2002, 106, 2994.
20. Winget, P.; Weber, E. J.; Cramer, C. J.; Truhlar D. G. Phys Chem Chem Phys 2000, 2, 1231.